

# CHOROIDAL VASCULARITY INDEX QUANTIFICATION IN GEOGRAPHIC ATROPHY USING BINARIZATION OF ENHANCED-DEPTH IMAGING OPTICAL COHERENCE TOMOGRAPHIC SCANS

GIUSEPPE GIANNACCARE, MD, PhD,\* MARCO PELLEGRINI, MD,\* STEFANO SEBASTIANI, MD,\* FEDERICO BERNABEI, MD,\* FABIANA MOSCARDELLI, CO,\* CLAUDIO IOVINO, MD,† PIETRO E. NAPOLI, MD,† EMILIO CAMPOS, MD\*

---

**Purpose:** To evaluate choroidal structural changes occurring over time in geographic atrophy (GA) secondary to age-related macular degeneration using choroidal vascular index (CVI).

**Methods:** Enhanced-depth imaging optical coherence tomography scans of 34 patients with GA and 32 control subjects were retrospectively analyzed. Data were collected at baseline and after a mean follow-up of  $18.3 \pm 8.3$  months. Choroidal images were binarized using the ImageJ software, and the luminal area and stromal area were segmented. Choroidal vascular index was defined as the ratio of luminal area to total choroid area.

**Results:** Patients with GA showed significantly lower values of CVI, total choroid area, luminal area, and subfoveal choroidal thickness compared to control subjects ( $65.83 \pm 3.95$  vs.  $69.33 \pm 3.11$ ,  $P < 0.001$ ;  $0.400 \pm 0.239$  mm<sup>2</sup> vs.  $0.491 \pm 0.132$ ,  $P = 0.006$ ;  $0.263 \pm 0.152$  mm<sup>2</sup> vs.  $0.340 \pm 0.094$ ,  $P = 0.002$ ;  $185.2 \pm 79.8$   $\mu$ m vs.  $216.8 \pm 58.8$   $\mu$ m,  $P = 0.036$ , respectively). Best-corrected visual acuity was significantly correlated only with choroidal thickness ( $R = -0.509$ ;  $P = 0.002$ ). During the follow-up period in patients with GA, subfoveal choroidal thickness decreased from  $185.2 \pm 79.8$  to  $152.2 \pm 73.1$  ( $P = 0.001$ ), stromal area increased from  $0.138 \pm 0.090$  mm<sup>2</sup> to  $0.156 \pm 0.068$  ( $P = 0.028$ ), and CVI decreased from  $65.83 \pm 3.95$  to  $62.24 \pm 3.63$  ( $P < 0.001$ ).

**Conclusion:** This study showed for the first time that CVI is reduced in patients with GA, and that this metric further worsened during the follow-up period.

RETINA 00:1–6, 2019

---

Age-related macular degeneration (AMD) is a leading cause of legal blindness among elderly individuals, especially in developed countries.<sup>1</sup> Geographic atrophy (GA) represents a common late-stage manifestation of AMD, and is characterized by progressive and irreversible loss of photoreceptors, retinal

pigment epithelium, and choriocapillaris within the macular region.<sup>2,3</sup> The choroidal structure is of particular interest in AMD pathogenesis because abnormalities of the choroidal circulation seem to play a primary role in its development and evolution.<sup>4,5</sup> Thanks to the improvements in optical coherence tomography (OCT) technology, such as enhanced-depth imaging (EDI) and swept-source OCT, a better visualization of the choroid structure along with a more accurate calculation of multiple quantitative and quantitative parameters is now feasible.<sup>6</sup> Among these, the measurement of choroidal thickness (CT) has gained increasing popularity in the recent years; however, it seems to be influenced by several biological variables (e.g., axial length, refractive error, intraocular pressure,

---

From the \*Ophthalmology Unit, S.Orsola-Malpighi University Hospital, University of Bologna, Bologna, Italy; and †Department of Surgical Sciences, Eye Clinic, University of Cagliari, Cagliari, Italy.

None of the authors has any financial/conflicting interests to disclose.

G. Giannaccare and M. Pellegrini authors contributed equally to the work and should be considered co-first Authors.

Reprint requests: Marco Pellegrini, MD, Ophthalmology Unit, S.Orsola-Malpighi University Hospital, University of Bologna, Via Palagi 9, 40138 Bologna, Italy; e-mail: marco.pellegrini@hotmail.it

and systolic blood pressure)<sup>7,8</sup> and represents a crude parameter that does not give information on the changes of the vascular and stromal choroidal components.

To overcome these limitations, the recent introduction of image binarization tools applied on EDI-OCT scans allowed to separately analyze and quantify the choroidal vascular and stromal structures.<sup>9,10</sup> In particular, choroidal vascularity index (CVI), measured by calculating the proportion of the luminal area (LA) to the cross-sectional choroid area, is a novel metric that can possibly be used as surrogate marker for monitoring retinal disease.<sup>11–18</sup>

The purpose of this study was to evaluate for the first-time CVI in the setting of GA secondary to AMD, and to further correlate this parameter with anatomical and functional measures.

### Materials and Methods

This retrospective cohort study included patients visited at the Retina Service of our Institution (S.Orsola-Malpighi University Hospital, Bologna, Italy) in the period between May 2016 and October 2018. Patients older than 55 years with a diagnosis of GA secondary to AMD, who underwent at least 2 complete ophthalmological examinations during the study period, were considered eligible. Sex- and age-matched control subjects without any sign of AMD on both fundus autofluorescence (FAF) and OCT scans were included as a control group. Exclusion criteria for both groups were media opacities that could influence image quality, the presence or history of choroidal neovascularization or any other retinal diseases (e.g., diabetic retinopathy, retinal dystrophy, and central serous chorioretinopathy), history of retinal laser and surgery, glaucoma, refractive error  $\geq 3$  diopters (D) spherical equivalent, and missing data from medical records. In case of previous cataract surgery, spherical equivalent before surgery must have fulfilled this criterion. If both eyes were eligible, the right eye was selected as the study eye. The study was performed in accordance with the principles of the Declaration of Helsinki and was approved by the local institutional review board.

The following data were extrapolated from medical records: age, sex, best-corrected visual acuity (BCVA) in Snellen and logMAR, lens status, fundus examination, color fundus images, FAF images, and spectral domain OCT scans with EDI mode.

Fundus autofluorescence images and EDI-OCT scans were obtained using the Spectralis HRA-OCT (Heidelberg Engineering, Heidelberg, Germany). Unifocal or multifocal areas of reduced FAF signal were

outlined using the RegionFinder function on the proprietary image analysis software (Heidelberg Eye Explorer, Heidelberg Engineering, Germany) to measure the size of GA areas. The total area was then automatically calculated using the software for each single image.<sup>19</sup>

Spectral domain OCT images were acquired with EDI mode using a volume scan of  $30^\circ \times 20^\circ$  containing 25 B-scans and centered on the macular region. Individual B-scan was 8.5 mm in length, spaced 240  $\mu\text{m}$  apart from each other and was an average of 30 frames. The OCT scan centered across the central foveal region with the thinnest retina was chosen for the analysis. The choroid was defined as the space between the outer border of the retinal pigment epithelium and the choroidal–scleral junction. Scans with poor quality or poorly visible choroidal scleral junction were excluded. Enhanced-depth imaging OCT scans were all obtained almost at the same time of the day, during the daily clinical activity. The subfoveal CT was measured manually by two independent examiners (M.P. and S.S.) using the caliper function tool of the image analysis software. The mean of the two measurements was used for the analysis.

The OCT images were binarized and segmented by the same examiners using the public domain software ImageJ 1.51s (National Institutes of Health, Bethesda, MD), with a semiautomated method previously described.<sup>11</sup> Briefly, the OCT image was opened in ImageJ (Figure 1, A and B), and the polygon tool was used to select the region of interest across the entire length of the OCT scan. The upper boundary of the region of interest was traced along the choroidal–retinal pigment epithelium junction and the lower boundary along the choroidal–scleral junction to identify the total choroidal area (TCA). After conversion to an 8-bit image, Niblack's autocal threshold was applied to binarized the image and demarcate the LAs and stromal areas (SAs) (Figure 1, C and D). The image was converted back to a red, green, blue image, and the color threshold tool was used to select the dark pixels, representing the LA (Figure 1, E and F). The TCA and LA were measured. The SA was calculated by subtracting LA from TCA. The CVI, defined as the LA divided by the TCA, was then computed.

Data analysis was conducted with SPSS statistical software (SPSS Inc, Chicago, IL). Values are expressed as mean  $\pm$  SD. The Shapiro–Wilk test was used to assess normality of data, and the Levene test was used to assess the homogeneity of variances. An independent-sample *t*-test was used to compare normally distributed variables between patients and control subjects, whereas the Mann–Whitney *U* test was

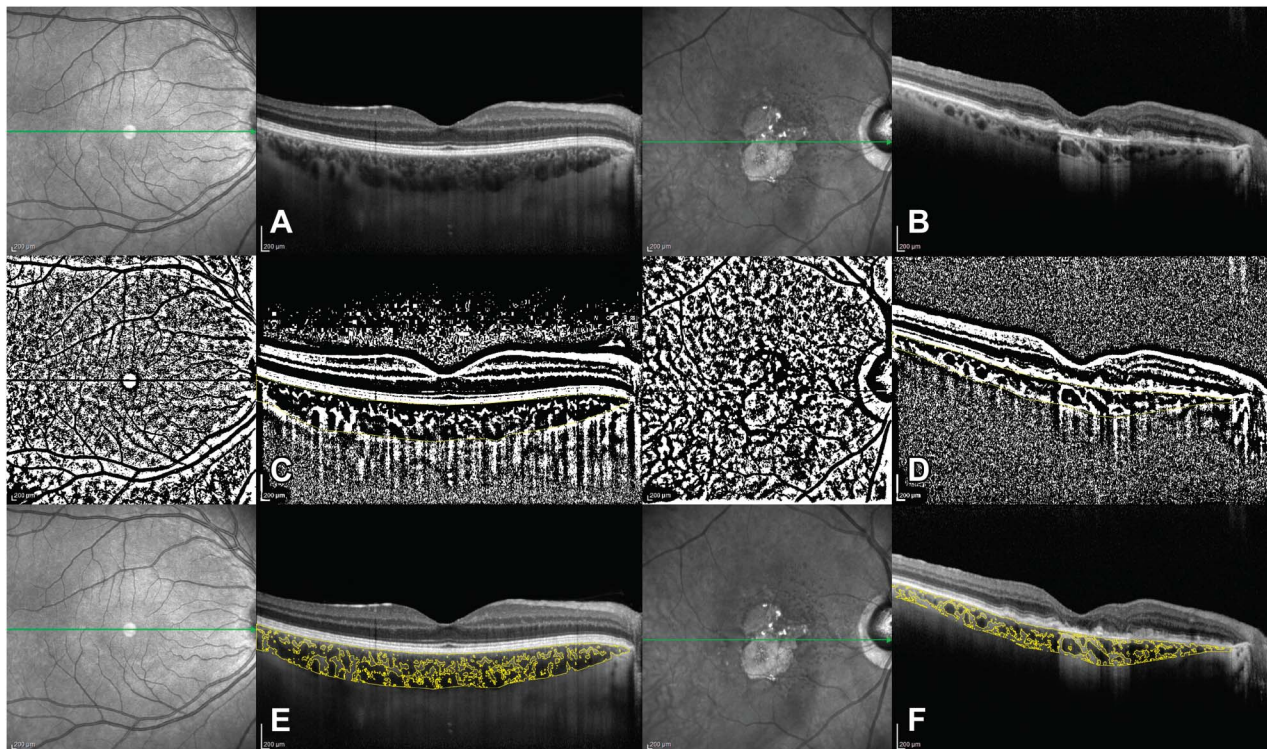


**Fig. 1.** Choroidal vascularity index calculation in a representative control subject (A, C, and E) and a representative patient with GA (B, D, and F). A and B. Original EDI-OCT images. C and D. Choroidal boundaries were traced to identify the TCA (yellow lines), and the images were binarized. E and F. The color threshold tool was used to select the dark pixels, representing the LA. The CVI was computed dividing LA by TCA.

used for not normally distributed variables. Changes of continuous variables during the follow-up period were analyzed using the Wilcoxon signed-rank test. The correlations of subfoveal CT and CVI with demographic and clinical parameters were examined using the Pearson correlation analysis. A *P* value <0.05 was considered statistically significant.

**Results**

Thirty-four eyes of 34 patients with GA secondary to AMD and 32 eyes of 32 control subjects were included in the study. The baseline demographic and clinical characteristics of patients with GA and control subjects are reported in Table 1. There was no significant difference in the mean age (*P* = 0.250) and sex distribution (*P* = 0.339) between the two groups. Mean BCVA was 0.87 ± 0.62 logMAR (20/148 Snellen) in patients with GA and 0.04 ± 0.06 logMAR (20/22 Snellen) in control subjects, and the difference was statistically significant (*P* < 0.001). The mean area of GA measured with FAF was 5.65 ± 5.13 mm<sup>2</sup> in patients with GA, whereas none of the controls had areas of chorioretinal atrophy. Subfoveal CT was significantly lower in patients with GA compared to

control subjects (185.2 ± 79.8 μm vs. 216.8 ± 58.8; *P* = 0.036).

Baseline choroidal parameters measured using the image binarization protocol in patients with GA and in control subjects are reported in Table 2. Total choroidal area, LA, and CVI were significantly reduced in patients with GA compared to control subjects (respectively, 0.400 ± 0.239 mm<sup>2</sup> vs. 0.491 ± 0.132, *P* = 0.006; 0.263 ± 0.152 mm<sup>2</sup> vs. 0.340 ± 0.094, *P* = 0.002; and 65.83 ± 3.95 mm<sup>2</sup> vs. 69.33 ± 3.11, *P* < 0.001). On the contrary, SA did not significantly differ between the two groups (*P* > 0.05). Choroidal vascularity index was not correlated with age, sex, and GA area (always *P* > 0.05).

Table 1. Baseline Characteristics of Patients With GA and Control Subjects

Characteristic	GA Group	Control Group
Patients (n)	34	32
Sex (m:f)	10:24	13:19
Age (years)	76.4 ± 8.9	73.9 ± 8.3
Phakic (n)	18	20
BCVA (Snellen)	20/148	20/22
BCVA (logMAR)	0.87 ± 0.62	0.04 ± 0.06
Area of GA (mm <sup>2</sup> )	5.65 ± 5.13	—
Subfoveal CT (μm)	185.2 ± 79.8	216.8 ± 58.8

Table 2. Choroidal Parameters Obtained With the Image Binarization Protocol in Patients With GA and Control Subjects

Characteristic	GA Group	Control Group	<i>P</i>
TCA (mm <sup>2</sup> )	0.400 ± 0.239	0.491 ± 0.132	<b>0.006</b>
LA (mm <sup>2</sup> )	0.263 ± 0.152	0.340 ± 0.094	<b>0.002</b>
SA (mm <sup>2</sup> )	0.138 ± 0.090	0.151 ± 0.042	0.092
CVI (LA/TCA)	65.83 ± 3.95	69.33 ± 3.11	<b>&lt;0.001</b>

Significant *P* values (< 0.05) are in bold.

Best-corrected visual acuity showed a significant correlation with subfoveal CT ( $R = -0.509$ ;  $P = 0.002$ ) and with GA area ( $R = 0.612$ ;  $P < 0.001$ ), but not with CVI ( $P > 0.05$ ).

Values of BCVA, area of GA, and all choroidal parameters collected in patients with GA after a mean follow-up period of  $18.3 \pm 8.3$  months (range 9–29 months) were also reviewed. Subfoveal CT significantly decreased from the baseline value of  $185.2 \pm 79.8 \mu\text{m}$  to  $152.2 \pm 73.1$  ( $P = 0.001$ ), and mean area of GA significantly increased from  $5.65 \pm 5.13 \text{ mm}^2$  to  $6.29 \pm 4.50$  ( $P < 0.001$ ), whereas BCVA did not change significantly ( $P > 0.05$ ). In addition, SA increased from  $0.138 \pm 0.090 \text{ mm}^2$  to  $0.156 \pm 0.068$  ( $P = 0.028$ ), CVI decreased from  $65.83 \pm 3.95$  to  $62.24 \pm 3.63$  ( $P < 0.001$ ), whereas no significant changes of TCA and LA were observed (both  $P > 0.05$ ) (Figure 2).

## Discussion

Changes in the choroidal structure and physiology are considered important mechanisms involved in the pathogenesis of AMD.<sup>20</sup> Ex vivo histopathological studies reported loss of choriocapillaris and decreased choroidal vascular density in eyes with GA.<sup>21,22</sup> Furthermore, reduced choroidal blood flow has been documented also by means of fluorescein angiography and indocyanine green angiography,<sup>23</sup> laser Doppler flowmetry,<sup>24</sup> and wavelet augmented B-scan ultrasonography.<sup>25</sup>

Ocular coherence tomography is considered the reference standard imaging method to diagnose and stage GA.<sup>26</sup> In this study, we used a novel tool applied on EDI-OCT images to investigate the vascular status of the choroid in both patients with GA secondary to AMD and healthy matched control subjects. This semiautomated tool permits to calculate four different parameters related to the conditions of the stromal and vascular components of the choroid, namely TCA, LA, SA, and CVI.<sup>10</sup>

We found that TCA, LA, and CVI values were lower in patients with GA compared to control subjects. Because CVI represents the proportion of LA to TCA, its reduction occurs in the presence of a higher reduction of LA (numerator of the ratio) compared with TCA (denominator). This phenomenon

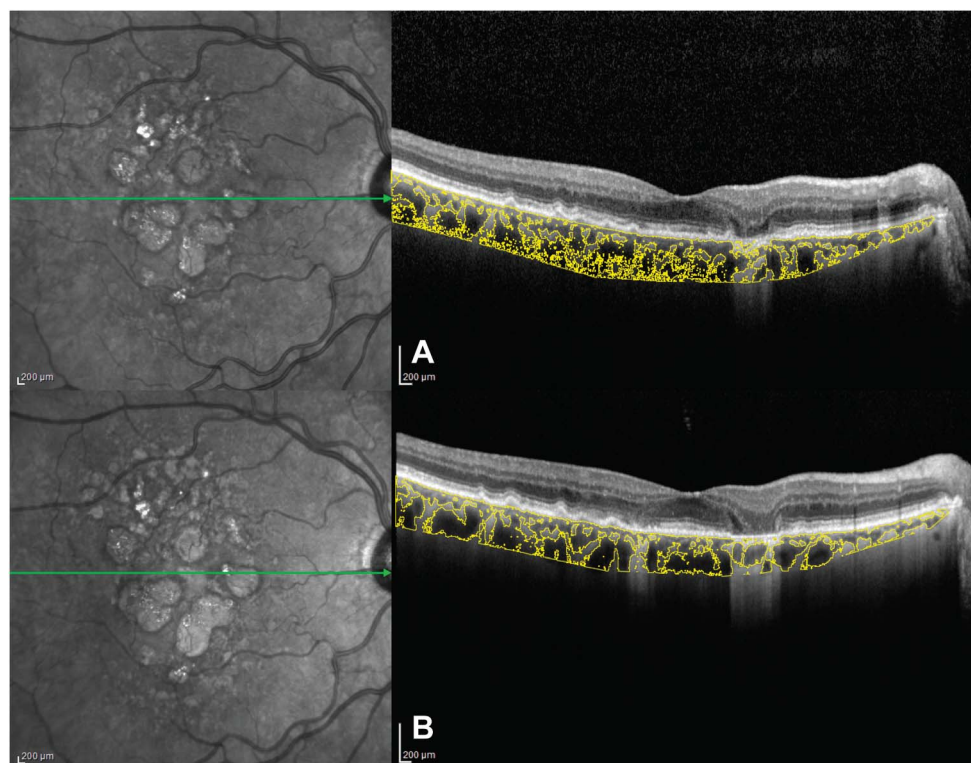


**Fig. 2.** Enhanced-depth imaging OCT in a representative patient with GA at baseline (A) and after 22 months (B). Choroidal vascularity index calculated with the OCT images binarization algorithm was 0.68 at baseline (A) and decreased to 0.65 after the follow-up (B).

may be explained by a more pronounced reduction of the vascular network of the choroid compared with the stromal tissue. In addition, we also evaluated the longitudinal changes of choroidal parameters over time in patients with GA. In particular, we observed a further reduction of the CVI and an increase of SA after the follow-up period compared with baseline values. Despite the cause–effect relationship between choroidal vascular abnormalities and retinal atrophy onset and/or progression could not be ascertained from this *in vivo* imaging technique, our findings further support the presence of choroidal vascular dysfunction in the setting of GA.

To the best of our knowledge, the current study provides the first analysis of CVI in the setting of GA secondary to AMD. Our results are consistent with those obtained from other studies in patients with earlier stages of dry AMD, different forms and stages of exudative AMD, and even in the fellow clinically nonaffected eye of the same patients.<sup>14–17</sup>

It is already known that the exudative and nonexudative types of AMD show different patterns of choroidal vascular changes over the course of the disease, with choroidal ischemia being present in nonexudative AMD, and enhanced blood supply in exudative AMD.<sup>25</sup> The only previous study that attempted to analyze the choroidal vascular changes in both the types of AMD reported a statistically significant reduction of CVI, without any difference between the two subgroups.<sup>17</sup> To exclude possible confounding factors derived from these two different subsets, we included in our analysis only patients with GA secondary to nonexudative AMD, providing the first quantification of choroidal vascular changes in this condition.

Corvi et al evaluated choroidal structure in patients with drusen and reticular pseudodrusen. Although CVI did not change between the two groups, a more pronounced reduction of TCA, LA, and SA was found in the reticular pseudodrusen group.<sup>27</sup> This finding suggests that alterations of the choroid structure occur in AMD since its early stages. Recently, Invernizzi et al<sup>18</sup> described an increase of CVI values in eyes with inactive AMD, which developed later an active stage of the disease, whereas no changes were observed in eyes that did not develop choroidal neovascularization over the entire follow-up period. Geographic atrophy and choroidal neovascularization can occur simultaneously in the same eye, with GA occurring first in most cases.<sup>28</sup> Therefore, serial CVI measurement might be a useful tool to potentially predict the development of active choroidal neovascularization in patients with GA.

Choroidal thickness represents another parameter commonly used to assess choroidal status in the setting

of various retinal and choroidal diseases, including GA. In our work, a reduction of CT was observed in patients with GA compared to controls, in agreement with previous studies.<sup>29–31</sup> However, this parameter measures the thickness at a single point of the choroid on vertical and horizontal scans, providing partial information, particularly in cases of fovea-sparing GA.<sup>32</sup> Conversely, CVI seems to be a more useful parameter providing insight into choroidal status, thanks to the quantitative assessment of the different structural components on a wider choroidal portion.

The present technique evaluated the entire choroidal layer and did not separately analyze the choriocapillaris, the medium choroidal vessel layer (Sattler's layer), and the large choroidal vessel layer (Haller's layer), and this issue represents the major limitation of the study, along with its retrospective nature and the variable follow-up. Future advances would allow to automatically detect and differentially analyze these layers to provide deeper insight on their involvement during the progression of the disease.<sup>33</sup> However, patients examined in our study were affected by late-stage nonexudative AMD, and this aspect might hamper to clearly identify and separate each layer.

In conclusion, the binarization of EDI-OCT choroidal images allowed to distinguish patients with GA from control subjects. This study showed for the first time that CVI, along with the TCA and the LA, are reduced in this subset of patients. In addition, CVI further worsened over the follow-up period in patients with GA.

**Key words:** age-related macular degeneration, geographic atrophy, choroidal vascularity index, optical coherence tomography.

## References

1. Klein R, Cruickshanks KJ, Nash SD, et al. The prevalence of age-related macular degeneration and associated risk factors. *Arch Ophthalmol* 2010; 128:750–758.
2. Boyer DS, Schmidt-Erfurth U, van Lookeren Campagne M, et al. The pathophysiology of geographic atrophy secondary to age-related macular degeneration and the complement pathway as a therapeutic target. *Retina* 2017;37:819–835.
3. Wright CB, Ambati J. Dry age-related macular degeneration pharmacology. *Handb Exp Pharmacol* 2017;242:321–336.
4. Grunwald JE, Metelitsina TI, Dupont JC, et al. Reduced foveolar choroidal blood flow in eyes with increasing AMD severity. *Invest Ophthalmol Vis Sci* 2005;46:1033–1038.
5. Pournaras CJ, Logean E, Riva CE, et al. Regulation of subfoveal choroidal blood flow in age-related macular degeneration. *Invest Ophthalmol Vis Sci* 2006;47:1581–1586.
6. Margolis R, Spaide RF. A pilot study of enhanced depth imaging optical coherence tomography of the choroid in normal eyes. *Am J Ophthalmol* 2009;147:811–815.
7. Gupta P, Jing T, Marziliano P, et al. Distribution and determinants of choroidal thickness and volume using automated seg-

- mentation software in a population-based study. *Am J Ophthalmol* 2015;159:293–301.
8. Sansom LT, Suter CA, McKibbin M. The association between systolic blood pressure, ocular perfusion pressure and subfoveal choroidal thickness in normal individuals. *Acta Ophthalmol* 2016;94:e157–e158.
  9. Sonoda S, Sakamoto T, Yamashita T, et al. Luminal and stromal areas of choroid determined by binarization method of optical coherence tomographic images. *Am J Ophthalmol* 2015;159:1123–1131.e1.
  10. Agrawal R, Gupta P, Tan KA, et al. Choroidal vascularity index as a measure of vascular status of the choroid: measurements in healthy eyes from a population-based study. *Sci Rep* 2016;6:21090.
  11. Agrawal R, Salman M, Tan KA, et al. Choroidal vascularity index (CVI)—a novel optical coherence tomography parameter for monitoring patients with panuveitis? *PLoS One* 2016;11:e0146344.
  12. Agrawal R, Chhablani J, Tan KA, et al. Choroidal vascularity index in central serious chorioretinopathy. *Retina* 2016;36:1646–1651.
  13. Rizzo S, Savastano A, Finocchio L, et al. Choroidal vascularity index changes after vitreomacular surgery. *Acta Ophthalmol* 2018;96:e950–e955.
  14. Sonoda S, Sakamoto T, Yamashita T, et al. Choroidal structure in normal eyes and after photodynamic therapy determined by binarization of optical coherence tomographic images. *Invest Ophthalmol Vis Sci* 2014;55:3893–3899.
  15. Wei X, Ting DSW, Ng WY, et al. Choroidal vascularity index: a novel optical coherence tomography based parameter in patients with exudative age-related macular degeneration. *Retina* 2017;37:1120–1125.
  16. Bakthavatsalam M, Ng DS, Lai FH, et al. Choroidal structures in polypoidal choroidal vasculopathy, neovascular age-related maculopathy, and healthy eyes determined by binarization of swept source optical coherence tomographic images. *Graefes Arch Clin Exp Ophthalmol* 2017;255:935–943.
  17. Koh LHL, Agrawal R, Khandelwal N, et al. Choroidal vascular changes in age-related macular degeneration. *Acta Ophthalmol* 2017;95:e597–e601.
  18. Invernizzi A, Benatti E, Cozzi M, et al. Choroidal structural changes correlate with neovascular activity in neovascular age related macular degeneration. *Invest Ophthalmol Vis Sci* 2018;59:3836–3841.
  19. Schmitz-Valckenberg S, Brinkmann CK, Alten F, et al. Semi-automated image processing method for identification and quantification of geographic atrophy in age-related macular degeneration. *Invest Ophthalmol Vis Sci* 2011;52:7640–7646.
  20. Zarbin MA. Current concepts in the pathogenesis of age-related macular degeneration. *Arch Ophthalmol* 2004;122:598–614.
  21. Spraul CW, Lang GE, Grossniklaus HE. Morphometric analysis of the choroid, Bruch's membrane, and retinal pigment epithelium in eyes with age-related macular degeneration. *Invest Ophthalmol Vis Sci* 1996;37:2724–2735.
  22. McLeod DS, Grebe R, Bhutto I, et al. Relationship between RPE and choriocapillaris in age-related macular degeneration. *Invest Ophthalmol Vis Sci* 2009;50:4982–4991.
  23. Pauleikhoff D, Spital G, Radermacher M, et al. A fluorescein and indocyanine green angiographic study of choriocapillaris in age-related macular disease. *Arch Ophthalmol* 1999;117:1353–1358.
  24. Grunwald JE, Hariprasad SM, DuPont J, et al. Foveolar choroidal blood flow in age-related macular degeneration. *Invest Ophthalmol Vis Sci* 1998;39:385–390.
  25. Coleman DJ, Silverman RH, Rondeau MJ, et al. Age-related macular degeneration: choroidal ischaemia?. *Br J Ophthalmol* 2013;97:1020–1023.
  26. Sadda SR, Guymer R, Holz FG, et al. Consensus definition for atrophy associated with age-related macular degeneration on OCT. *Ophthalmol* 2018;125:537–548.
  27. Corvi F, Souied EH, Capuano V, et al. Choroidal structure in eyes with drusen and reticular pseudodrusen determined by binarisation of optical coherence tomographic images. *Br J Ophthalmol* 2017;101:348–352.
  28. Kaszubski P, Ben Ami T, Saade C, et al. Geographic atrophy and choroidal neovascularization in the same eye: a review. *Ophthalmic Res* 2016;55:185–193.
  29. Adhi M, Lau M, Liang MC, et al. Analysis of the thickness and vascular layers of the choroid in eyes with geographic atrophy using spectral-domain optical coherence tomography. *Retina* 2014;34:306–312.
  30. Lee JY, Lee DH, Lee JY, Yoon YH. Correlation between subfoveal choroidal thickness and the severity or progression of nonexudative age-related macular degeneration. *Invest Ophthalmol Vis Sci* 2013;54:7812–7818.
  31. Lindner M, Bezatis A, Czauderna J, et al. Choroidal thickness in geographic atrophy secondary to age-related macular degeneration. *Invest Ophthalmol Vis Sci* 2015;56:875–882.
  32. Schmitz-Valckenberg S, Fleckenstein M, Helb HM, et al. In vivo imaging of foveal sparing in geographic atrophy secondary to age-related macular degeneration. *Invest Ophthalmol Vis Sci* 2009;50:3915–3921.
  33. Uppugunduri SR, Rasheed MA, Richhariya A, et al. Automated quantification of Haller's layer in choroid using swept-source optical coherence tomography. *PLoS One* 2018;13:e0193324.